Capacity of Cell Clusters with Coordinated Processing

Alessandro Vanelli-Coralli
DEIS/ARCES –
University of Bologna, Italy,
avanelli@deis.unibo.it

Roberto Padovani
Qualcomm Inc.,
San Diego, CA, US
rpadovani@qualcomm.com

Jilei Hou
Qualcomm Inc.,
San Diego, CA, US
jhou@qualcomm.com

John E. Smee
Qualcomm Inc.,
San Diego, CA, US
jsmee@qualcomm.com

***Abstract*—The potential capacity gains of coordinated processing in the reverse link of a cellular system are evaluated. Three different matched filter-based receiver schemes, successive intra-cell interference cancellation, successive intra- and inter-cell interference cancellation, and centralized successive interference cancellation, are analyzed considering different path loss exponents and various limiting factors such as non-detectable paths and imperfect interference cancellation. Performance of the three schemes is compared to that achievable by the single user matched filter receiver and by the optimum joint decoding scheme. Capacity gains ranging from 41% up to 183% over the classical single user matched filter receiver are highlighted.**

I. Introduction

In this paper, we focus on the reverse link of a cellular system adopting coordinated processing among the base stations belonging to a cell cluster. Coordinated processing can range from the exchange of the decoded data among base stations, to a complete centralized processing of the cluster users. The centralized processing has been analyzed from a theoretical point of view in many scientific works [1-4] and allows for the implementation of the joint decoding (JD) scheme, which is optimum, in terms of capacity, and provides an upper bound to all other multiuser decoding schemes [5].

The objective of our analysis is to identify the potential capacity gains of matched filter (MF) based receivers enforcing different interference cancellation strategies [6], according to the degree of coordination present in the system. In order to provide realistic estimates of the achievable capacity, various performance limiting factors, such as non-detectable paths and imperfect interference cancellation are considered. The evaluation is performed as a function of the path loss exponents. 3G networks rely in fact upon propagation induced cell isolation, provided by path loss and base station antenna patterns, to limit inter-cell interference. When the path loss exponent decreases, as may happen in dense cellular layouts, cell isolation reduces and inter-cell interference increases. Furthermore, when intra-cell interference cancellation techniques, that have been already proved sound and feasible [7], are applied, inter-cell interference becomes even more important, as it represents the major limiting factor for the capacity.

II. System Scenarios

We consider a cellular system with base stations placed at the center of each cell. Depending on the degree of coordination enforced in the system, the cell site may include: an isolated base station with A antennas; a base station with A antennas connected to all the other base stations in the cluster; a set of A antennas without base station functionalities linked to a centralized processing site. In the following, these three scenarios are described in detail.

A. Scenario A: Non-cooperative base stations

This scenario refers to the current 3G network layout, where the cell site is a full-fledged transmitting and receiving base station. In this scenario, a base station attempts to decode each user that has that base station in its active set. The same user can therefore be possibly decoded by many base stations. The number of base stations that can be listed in a user's active set, and thus the number of base stations that attempt to decode the user, is defined as a system parameter. In this scenario, no coordination among base stations is enforced: the first base station that successfully decodes the user sends the user data packet to the BSC and, through it, to the network. In this case, a base station has knowledge only of the data transmitted by the users it has successfully decoded. Intra-cell interference can be dealt with, but inter-cell interference cannot be eliminated. Notably, for a given base station inter-cell interference refers to the interference created by those users in whose active set list the base station is not listed. In this paper, we will assume that the user active set consists of a single base station; therefore, intra-cell interference refers to the interference created by the user at its serving base station, whereas inter-cell interference refers to the interference created by the user at all other base stations. We should point out that in this simplified analysis we do not take into account fast fading and soft-handoff.

B. Scenario B: Coordinated base station processing

This scenario represents an evolution of *Scenario A*. The cell site is still a full-fledged transmitting and receiving base station and the decoding procedure is the same as in *Scenario A*. However, once a base station has decoded a user, the user data packet is broadcasted, through high data rate links, to all

other base stations in the cluster. In this case, knowledge of the data transmitted by users in the neighboring cells is available at each base station in the cluster and the inter-cell interference caused by a user can be removed after the user decodes.

C. Scenario C: Centralized base station processing

The third scenario refers to a distributed antenna system: the cell sites are simple receiving and transmitting elements, and the base station signal processing is moved to a centralized site where every user of the cluster is decoded. The remote antennas are connected to the centralized base station with high data rate links capable of supporting the transmission of the signal samples. This scenario can be thought of as a system with a single isolated cell with a number of physically separated antennas equal to the total number of antennas deployed in the two previous scenarios.

III. System Model

The cell clusters consist of N_c cells, A antennas per cell, and K user per cell. Therefore, R=N_c A receivers, and T= N_c K independent transmitters are present in the system..

The received signal can be represented as

$$y = Hx' + w \tag{1}$$

where x is the ($1\times T$) row vector representing the transmitted symbols, y is the ($R\times 1$) column vector representing the received signal, w is the ($R\times 1$) column vector representing the complex Additive White Gaussian Noise (AWGN) with power spectral density N_0, and H is the (R×T) matrix representing the complex channel gains. The element, h_{jk}, of H represents the complex channel gain pertaining to the link between the kth transmitter and the jth antenna, and it is modeled as

$$h_{jk} = r_{jk}^{-m/2} 10^{\xi_{jk}/20} e^{j\theta_{jk}}, \tag{2}$$

where r_{jk} is the distance between the transmitter and the receiver, m is the path loss exponent, θ_{jk} is a random phase term assumed i.i.d. and uniformly distributed in [0, 2π[, and ξ_{jk} represents log-normal shadowing with standard deviation σ_S. The log-normal shadowing is modeled as recommended in [1]. The channel time variation is assumed slow with respect to the user transmission rate, so that H can be considered constant over the transmission of a data packet.

In order to consider the fact that in a real system a link between a transmitter k and an antenna j might be too low to be detected, the complex channel gain matrix entries are organized in two matrixes, B and D, according to a detectability criterion. An element b_{jk} of the matrix B is non zero and equal to h_{jk} if and only if h_{jk} is non-detectable; an element d_{jk} of the matrix D is non zero and equal to h_{jk} if and only if h_{jk} is detectable. In this analysis, the detectability criterion is defined with reference to each single user. For a given user k, h_{jk} is detectable if and only if

$$\left|h_{jk}\right| \geq \alpha \max_i \left\{\left|h_{ik}\right|\right\}, \quad 0 \leq \alpha \leq 1. \tag{3}$$

When (3) is not satisfied h_{jk} is non detectable and contributes to the background noise. According to (3), two extreme cases are possible, α=0, which means that every path is detectable, and α=1, which means that only the strongest path is detectable.

Furthermore, in *Scenario A* and *Scenario B*, the detectable links reaching a receiver may come from a cell user or from a neighbor cell user, therefore contributing to the intra- or inter-cell interference, respectively. To the end of including this difference within the mathematical model developed, the elements of the detectable link matrix D are separated in the two matrixes U and Y. An element u_{jk} of U is non zero and equal to d_{jk} if and only if the kth user is served by the base station utilizing the jth antenna; on the other hand, an element υ_{jk} of Y is non zero and equal to d_{jk} if and only if the kth user is not served by the base station utilizing the jth antenna. From the above discussion, it follows directly that

$$H = D + B = U + \Upsilon + B \tag{4}$$

At the base station side, we assume that a matched filter receiver is implemented either with or without successive interference cancellation. Although it is known that a minimum mean squared error (MMSE) receiver would have yield better performance, for the purpose of the comparison carried out in this paper, the MF approach has been deemed sufficient. In any case, ideal JD is always reported in the numerical results as a reference case.

In this framework, four different receiver schemes are considered. In *scenario A*, a matched filter receiver without interference cancellation (MF), and a matched filter receiver with successive intra-cell interference cancellation (MF-SI^{2}C) are possible. In *Scenario B*, by exploiting the coordination among base stations, i.e., the distributed knowledge of the data packet transmitted by neighbor cell users, inter-cell interference cancellation can be added to the receiver; hence a matched filter with successive intra-cell and inter-cell interference cancellation (MF-SI^{3}C) is considered. Finally, in the third scenario, *Scenario C*, the distinction between intra- and inter-cell interference vanishes and we consider a matched filter with successive interference cancellation (MF-SIC).

IV. System Capacity Analysis

The four approaches are compared in terms of the achievable total cell throughput they yield under the same assumptions. In particular, the i-th cell throughput is evaluated as

$$C_i = \sum_{k\in BS_i} \log_2\left(1+\frac{1}{\Gamma} SINR_k\right) \quad \text{[b/s/Hz]} \tag{5}$$

where BS_i is the set of the users served by the ith base station, $SINR_k$ is the signal to interference-plus-noise ratio (SINR) of

the *k*th user, which depends on the receiver scheme considered, and Γ is the back-off factor used to account for non-ideal forward error correction code performance. The results presented will assume $\Gamma=1$.

Assuming, without loss of generality, that users are labeled in increasing order of decoding, i.e., k=1 is the first user to be decoded, and k=T is the last user to be decoded, the SINR values achieved by the MF, MF-SI^{2}C, MF-SI^{3}C, and MF-SIC receivers are reported at the bottom of this page in (9), (10), (11), and (12), respectively. P_k represents the user transmitted power, I_R is the ($R\times R$) identity matrix, * is the transpose conjugate operator, and d_k, u_k, υ_k, b_k are the *k*th column vectors of matrixes D, U, *Y*, and *B*, respectively. The factor β that appears in (10), (11), and (12) represents the fraction of the interference power actually removed from the total interference and accounts for possible imperfect interference cancellation.

A key element for the analysis of the system capacity is the definition of the power distribution among users. Different power allocations yield in fact different results in term of total system throughput. Ideally, in order to enlarge the capacity region as much as possible, under the assumption of perfect interference cancellation, i.e., β=1, each user should be allowed to transmit at its maximum power. However, in real systems, other considerations, such as system fairness and power consumption, play a fundamental role, and a reasonable power allocation must be sought.

Since the main goal of this work is to identify the gains over a traditional system configuration achievable by allowing a certain degree of processing coordination among base stations, we adopted the power distribution that results from the application of the power control algorithm currently adopted in the 1xEV-DO system [9]. Under the assumption of invariant channel gains over a packet transmission, the power control algorithm is limited by the rise over thermal (RoT) control, where, at the *j*th antenna, RoT is defined as

$$RoT_j = \frac{N_0 + \sum_k P_k \mid h_{ik} \mid^2}{N_0}. \qquad (6)$$

The RoT control allows each user to transmit with a power level P_k to make the antenna RoT equal to a target value, e.g. RoT=6dB. As we will demonstrate, this imposes a constraint on the maximum achievable capacity for every approach.

V. Capacity upper bound

The JD capacity is the maximum achievable capacity and is given by [5]

$$C_{JD} = \log_2 \det\left(I_R + \frac{1}{N_0} H K_p H^* \right) \qquad (7)$$

where K_p=diag(P_1, P_2, …, P_T). Interestingly, (7) can be upper bounded by applying the Hadamard inequality as

$$C_{JD} \le \sum_{j=1}^{R} log_2(RoT_j). \qquad (8)$$

Eq. (8) gives an upper bound on the JD capacity, and hence on the maximum achievable capacity, in terms of the RoT constraint and the number of antennas: whatever power distribution is adopted the capacity upper bound scales linearly with the number of antennas and logarithmically with the RoT.

VI. Numerical Results

A hexagonal cellular layout with seven cells (N_c=7), two antennas per cell site (*A*=2) and twenty users per cell (K=20) is considered in the analysis. The target RoT is set to 6 dB per antenna, the path loss exponent varies in the range [2-5], and the cell radius, Δ, is a function of the path loss exponent through the following relationship:

$$SINR_k = P_k \frac{\| u_k \|^4}{u_k^* \left[\sum_{\ell=1,\ell\neq k}^{T} P_\ell u_\ell u_\ell^* + \sum_{\ell=1}^{T} P_\ell \upsilon_\ell \upsilon_\ell^* + \sum_{\ell=1}^{T} P_\ell b_\ell b_\ell^* + N_0 I_R \right] u_k} \qquad (9)$$

$$SINR_k = P_k \frac{\| u_k \|^4}{u_k^* \left[\sum_{\ell=1,\ell\neq k}^{T} P_\ell u_\ell u_\ell^* - \beta \sum_{\ell=1}^{k-1} P_\ell u_\ell u_\ell^* + \sum_{\ell=1}^{T} P_\ell \upsilon_\ell \upsilon_\ell^* + \sum_{\ell=1}^{T} P_\ell b_\ell b_\ell^* + N_0 I_R \right] u_k} \qquad (10)$$

$$SINR_k = P_k \frac{\| u_k \|^4}{u_k^* \left[\sum_{\ell=1,\ell\neq k}^{T} P_\ell u_\ell u_\ell^* - \beta \sum_{\ell=1}^{k-1} P_\ell u_\ell u_\ell^* + \sum_{\ell=1}^{T} P_\ell \upsilon_\ell \upsilon_\ell^* - \beta \sum_{\ell=1}^{k-1} P_\ell \upsilon_\ell \upsilon_\ell^* + \sum_{\ell=1}^{T} P_\ell b_\ell b_\ell^* + N_0 I_R \right] u_k} \qquad (11)$$

$$SINR_k = P_k \frac{\| d_k \|^4}{d_k^* \left[\sum_{\ell=1,\ell\neq k}^{T} P_\ell d_\ell d_\ell^* - \beta \sum_{\ell=1}^{k-1} P_\ell d_\ell d_\ell^* + \sum_{\ell=1}^{T} P_\ell b_\ell b_\ell^* + N_0 I_R \right] d_k} \qquad (12)$$

$$\Delta = \min(10^3; 10^{\frac{10.5}{m}}) \quad \text{[meters]} \tag{13}$$

The users are randomly dropped in the cellular layout according to a spatially uniform distribution. Given the user position the complex channel gains are computed, and the transmitting power level defined so as to satisfy the RoT constraint. Equations (5) and (7) are then numerically evaluated for each user drop. The average cell throughput is obtained by averaging (5) and (7) on different drops. Fig. 1 shows the relationship between the path loss exponent and the resulting inter-cell interference or reuse factor f. For increasing values of *m*, the *f* factor decreases, because of the higher isolation between cells.

Fig. 2 through Fig. 4 show the average throughput of the cluster central cell for the four different receivers, as a function of the inter-cell interference factor, *f*, [8]. The inter-cell interference factor is a function of the pair (m,Δ) and is evaluated numerically. The JD capacity, normalized to the number of cells, N_c, is also reported in each figure Interestingly, numerical evaluation shows that (8) is practically satisfied with the equality sign: with the RoT constraint set to 6 dB, the right hand side of (8), normalized to N_c, turns out to be 3.99.

In Fig. 2, the central cell throughput is reported in ideal conditions, i.e., perfect path detectability, α=0, perfect interference cancellation, β=1, and capacity achieving codes, Γ=1. Focusing on *Scenario A*, the intra-cell interference cancellation benefit is represented by the MF-SI^{2}C gain over MF. For decreasing values of the *f* factor, the capacity gain increases because the cell isolation increases and the impact of the inter-cell interference becomes marginal. Allowing the base stations to coordinate their processing, i.e., *Scenario B*, enables further gains as it is shown by the MF-SI^{3}C curve. In this case, the capacity gain of MF-SI^{3}C over MF-SI^{2}C increases for increasing values of *f*, because this corresponds to larger inter-cell interference, which is removed by MF-SI^{3}C but not by MF-SI^{2}C. Finally, the comparison between MF-SI^{3}C and MF-SIC, highlights the power gain benefit carried in by the adoption of centralized processing. The power gain increases for increasing values of *f* because the reduced isolation among cells makes the combining across the distributed antennas more useful

In Fig. 3, the effect of undetectable paths is investigated by considering α=0.1, i.e., for a given user, a path is undetectable, and contributes only to the background interference, when it is 10 dB or more below the strongest link. Notably, the path detectability has an impact only on the capacity of *Scenario B* and *Scenario C*, and it is immaterial for *Scenario A*, because we assumed single path propagation. By comparing the curves with α=0.1 to the curves with α=0 for the MF-SI^{3}C and MF-SIC approaches, it is apparent that undetectable paths are more detrimental for Scenario C. Undetectable paths cause in fact an increase in the background interference for both MF-SI^{3}C and MF-SIC, but also a loss in power gain for MF-SIC.

Fig. 4 deals with the effect of imperfect interference cancellation: the parameter β is set to 0.8, meaning that only 80% of intra- and inter-cell interference is removed for each decoded user. The major impact of the imperfect interference cancellation is clearly on the MF-SI^{3}C receiver. MF-SIC is still able to exploit the power gain coming from the centralized processing with *R* antennas.

The evaluation of the degradation due to the adoption of non-ideal codes, i.e., a back-off factor Γ larger than 1, is straightforward as with 20 users per cell the system is forced to work in the low SINR regimes, and hence the capacity scales almost linearly with the back-off factor for every approach.

The results discussed above have been obtained assuming the same RoT constraint for each receiver scheme, and were aimed at assessing the sensitiveness of the different approaches to the three limiting factors. However, when assessing the relative gains of one approach over the others, "*effective*" RoT control must be considered [7]: when interference cancellation is used, it is in fact sensible to impose the RoT constraint after the cancellation operation, thus leading to a more aggressive power allocation for the interference cancellation schemes. Adopting an effective RoT control does not change the general considerations made in the previous sections, and it allows getting an insight in the potential of the proposed approaches with respect to the single user MF approach.

To this aim, in Fig. 5, the central cell throughput is reported under the effective RoT control constraint, considering the combined degradation caused by the non-detectable paths and the imperfect interference cancellation. Focusing on the *f* values around 0.7, the intra-cell interference cancellation, MF-SI^{2}C, yields a 41% gain over the MF approach; the intra- and inter-cell interference cancellation, MF-SI^{3}C, adds another 53% gain; the MF-SIC brings in a 31% throughput gain with respect to MF-SI^{3}C, driving the total gain over MF to 183%.

VII. Conclusions

In this paper, we addressed the evaluation of the capacity of the reverse link of a cell cluster employing coordinated processing at the base station. Three scenarios and four different receivers have been studied showing that, by allowing the system complexity to increase, large capacity gains, from 41% up to 183% over uncoordinated single user MF scheme, can be achieved.

Acknowledgment

We would like to thank Prof. Jack Wolf for his continuous support and for the many fruitful discussions, and Prof. David Tse for pointing us to the Hadamard inequality used in (8).

REFERENCES

[1] S. V. Hanly and P. A. Whiting, "Information-theoretic capacity of multireceiver networks," *Telecommun. Syst.*, vol. 1, pp. 1–42, 1993.

[2] O. Popescu and C. Rose "Sum Capacity and TSC Bounds in Collaborative Multibase Wireless Systems" *IEEE Trans. on Inf. Theory*, vol. 50, Oct. 2004, pp. 2433-2438.

[3] L. Dai, S. Zhou, and Y. Yao "Capacity Analysis in CDMA Distributed Antenna Systems" *IEEE Trans. on Wireless Commun.*, vol. 4, Nov. 2005, pp.2613-2620.

[4] S. Zhou, M. Zhao, X. Xu, J. Wang, and Y. Yao, "Distributed Wireless Communication System: A New Architecture for Future Public Wireless Access," *IEEE Commun. Mag.*, vol. 41, Mar. 2003, pp. 108–113.

[5] David Tse and Pramod Viswanath *Fundamentals of Wireless Communication*, New York, Cambridge University Press, July 2005.

[6] J. G. Andrews, "Interference Cancellation for Cellular Systems: A Contemporary Overview" *IEEE Wireless Comm.* , April 2005, pp.19-29.

[7] J. Hou, J. E. Smee, H. Pfister, S. Tomasin "Implementing Interference Cancellation to Increase the EV-DO RevA Reverse Link Capacity", to appear in *IEEE Comm. Mag.* Feb. 2006.

[8] A.J. Viterbi, *Principles of Spread Spectrum Communications*, Addison Wesley, 1995.

[9] 3GGP2 CR.1002-0, "cdma2000 Evaluation Methodology", http:\\www.3gpp2.org

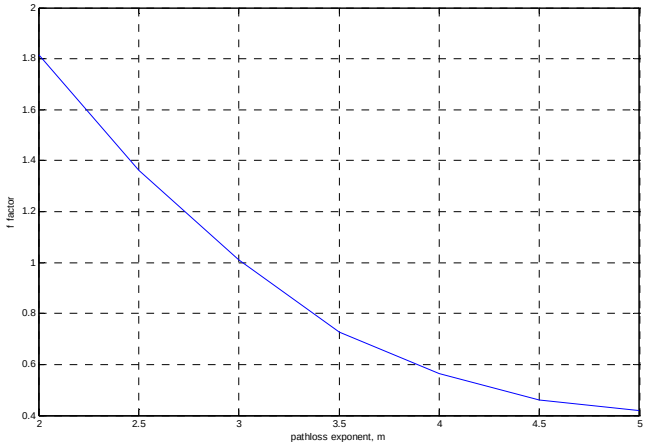

Fig. 1Inter-cell interference factor, f, vs. path loss exponent, m. RoT=6 dB.

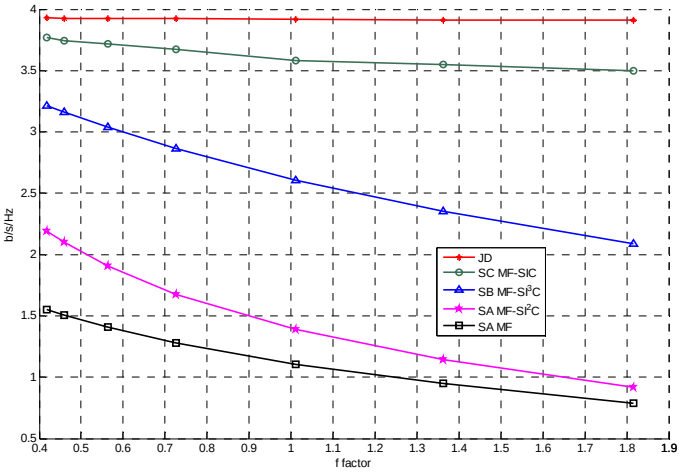

Fig. 2 Average central cell throughput [bit/s/Hz] vs. f factor; K=20, A=2, RoT=6dB per antenna, σ_S=8.9 dB, Nc=7, α=0, β=1, and Γ=1.

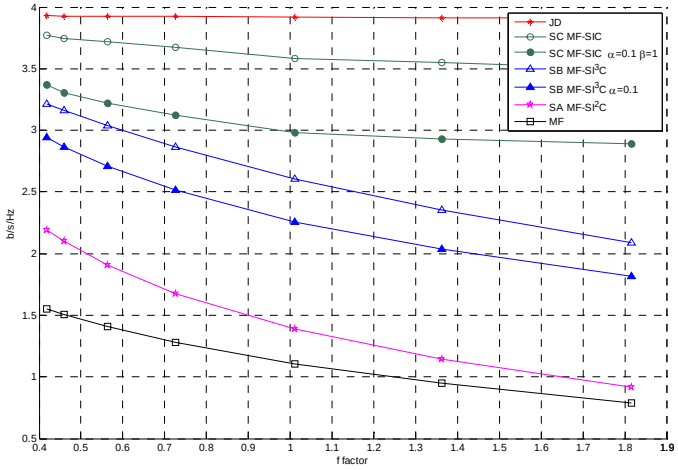

Fig. 3 Average central cell throughput [bit/s/Hz] vs. f factor; K=20, A=2, RoT=6dB per antenna, σ_S=8.9 dB, Nc=7, β=1, Γ=1, α=0 and α=0.1.

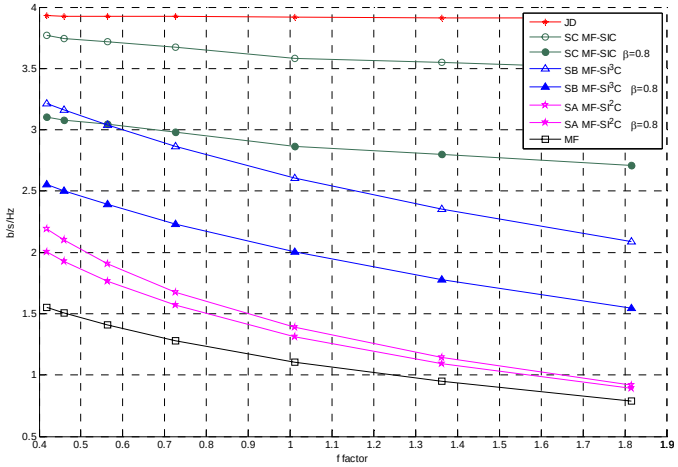

Fig. 4. Average central cell throughput [bit/s/Hz] vs. f factor; K=20, A=2, RoT=6dB per antenna, σ_S=8.9 dB, Nc=7, α=0, Γ=1, β=1, and β=0.8.

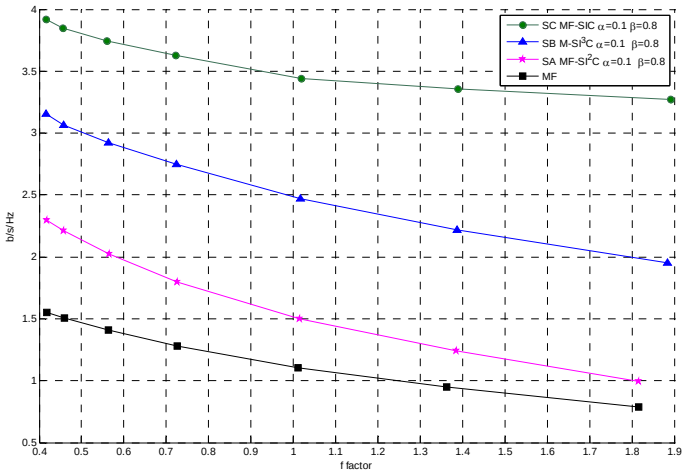

Fig. 5 Average central cell throughput [bit/s/Hz] vs. f factor; K=20, A=2, Effective RoT, σ_S=8.9 dB, Nc=7. Non-ideal cases, i.e., α=0.1, β=0.8, and Γ=1.